

# Chapter 3

## Bose-Einstein Condensation: The Theoretical Aspects

This chapter provides the elementary scope of Bose-Einstein condensation in the dilute weakly interacting Bose gas. First the noninteracting model was shown to predict that BEC can exist even in this limiting case. Also it guided the experimental physicists what to look for to confirm the realization of BEC. Next the interactions are included to show that, though weak they are, one gets better results compare with the ideal gas. From the interacting model, many features matched with experiment and new phenomena can be predicted using mean field approach.

### 3.1 Ideal Bose Gas in the Harmonic Trap

BEC in the harmonic trap is different from most of BEC written in text books, since the trapping potential considered here are inhomogeneous (spatially varying) potential. The system shows many interesting results. In almost all the experiments, the trap used can be approximated by harmonic potential [38]

$$V_{\text{ext}}(\mathbf{r}) = \frac{m}{2}(\omega_x^2 x^2 + \omega_y^2 y^2 + \omega_z^2 z^2), \quad (3.1)$$

with the energy eigenvalue

$$\varepsilon_{n_x n_y n_z} = \left(n_x + \frac{1}{2}\right) \hbar\omega_x + \left(n_y + \frac{1}{2}\right) \hbar\omega_y + \left(n_z + \frac{1}{2}\right) \hbar\omega_z, \quad (3.2)$$

and the ground state wavefunction of free particle in the harmonic trap can be described by

$$\phi_0(\mathbf{r}) = \left(\frac{m\omega_{\text{ho}}}{\pi\hbar}\right)^{3/4} \exp\left[-\frac{m}{2\hbar}(\omega_x x^2 + \omega_y y^2 + \omega_z z^2)\right], \quad (3.3)$$

where

$$\omega_{\text{ho}} = (\omega_x \omega_y \omega_z)^{1/3}.$$

Then the ground state wavefunction of  $N$  noninteracting particles is

$$\Phi_N(\mathbf{r}_1, \dots, \mathbf{r}_N) = \prod_{i=1}^N \phi_0(\mathbf{r}_i). \quad (3.4)$$

The density distribution is obtained from

$$n(\mathbf{r}) = N |\phi_0(\mathbf{r})|^2, \quad (3.5)$$

and the size of the cloud is determined not by  $N$  but the characteristic length scale

$$a_{\text{ho}} = \left(\frac{\hbar}{m\omega_{\text{ho}}}\right)^{1/2} \quad (3.6)$$

which corresponds to the average width of the Gaussian wavefunction Eq. (3.3).

At finite temperature some of the atoms are being thermally distributed in the excited state. The radius of the thermal cloud is larger than  $a_{\text{ho}}$ . The rough estimation is done by assuming that  $k_B T \gg \hbar\omega_{\text{ho}}$  and using Boltzmann distribution

$$n_d(\mathbf{r}) \propto \exp\{-V_{\text{ext}}(\mathbf{r})/k_B T\}. \quad (3.7)$$

Choosing external potential to be

$$V_{\text{ext}}(\mathbf{r}) = \frac{m\omega_{\text{ho}}^2 r^2}{2}, \quad (3.8)$$

the width of Gaussian is

$$R_T = a_{\text{ho}}(k_B T/\hbar\omega_{\text{ho}})^{1/2}, \quad (3.9)$$

hence larger than  $a_{ho}$ . Using Bose-Einstein distribution doesn't change significantly this estimation.

To obtain momentum distribution the ground state wave functions are Fourier transformed to give

$$\phi_o(\mathbf{k}) = \int \frac{d\mathbf{r}}{(2\pi\hbar)^3} \phi_o(\mathbf{r}) e^{i\mathbf{k}\cdot\mathbf{r}}, \quad (3.10)$$

and the peak in momentum space is centered at zero momentum and having a width proportional to  $a_{ho}^{-1}$ . The thermal cloud also spread in momentum space.

Eq. (3.5) predicts that BEC will show up with the appearance of the sharp peak in density distribution. This feature is different from the uniform case where the peak will show up only in momentum space, not in coordinate space, since the condensed and noncondensed particles fill the same volume.

The trap can be spherical or cylindrical symmetry. In the case of axial symmetry, the parameter  $\lambda$  which defined to be

$$\lambda = \omega_z/\omega_{\perp}, \quad (3.11)$$

where  $\omega_{\perp}, \omega_z$  are radial and axial frequency. The asymmetry of the trap force has an advantage for giving further evidence of Bose-Einstein condensation from the analysis of the momentum distribution. From Eq. (3.10) the average of axial and radial width can be obtain. Their ratio is

$$\begin{aligned} \sqrt{\langle p_z^2 \rangle / \langle p_{\perp}^2 \rangle} &= \sqrt{\lambda} \\ &= \sqrt{\langle x^2 \rangle / \langle z^2 \rangle}, \end{aligned} \quad (3.12)$$

called *aspect ratio*, is fixed by asymmetry parameter.

The condensate cloud in  $x - z$  plane is an ellipse. Instead the noncondensate (thermal) cloud should be spherical, since they obey the equipartition principle. This feature has been interpreted from the beginning as an important signature of BEC [23, 29, 30].

From Bose-Einstein distribution, the total number of particles is given by

$$N = \sum_{n_x, n_y, n_z} (\exp\{\beta(\varepsilon_{n_x n_y n_z} - \mu)\} - 1)^{-1}, \quad (3.13)$$

where  $\mu$  is classical potential and  $\beta \equiv 1/k_B T$ . When the BEC occurs the chemical potential is equal to the lowest state energy or

$$\mu_c = \frac{3}{2} \hbar \bar{\omega}, \quad (3.14)$$

where  $\bar{\omega} = (\omega_x + \omega_y + \omega_z)/3$  is arithmetic average of the trapping frequency. Apparently the lowest state occupation diverges so this term must be separated out. Then

$$N - N_0 = \sum_{n_x, n_y, n_z \neq 0} \frac{1}{\exp\{\beta \hbar (\omega_x n_x + \omega_y n_y + \omega_z n_z)\} - 1}. \quad (3.15)$$

Assuming that the level spacing becomes smaller and smaller the sum can be replaced by an integral

$$N - N_0 = \int_0^\infty dn_x dn_y dn_z \frac{1}{\exp\{\beta \hbar (\omega_x n_x + \omega_y n_y + \omega_z n_z)\} - 1}. \quad (3.16)$$

This assumption corresponds to a semiclassical approximation for excited state and is good under conditions that  $N$  is large and  $k_B T \gg \hbar \omega_{ho}$ .

Integrating Eq. (3.16) gives

$$N - N_0 = \zeta(3) \left( \frac{k_B T}{\hbar \omega_{ho}} \right)^3 \quad (3.17)$$

where  $\zeta(n)$  is the Riemann zeta function. To obtain the transition temperature, imposing that  $N_0 \rightarrow 0$  at the transition, then

$$\begin{aligned} k_B T_c &= \hbar \omega_{\text{ho}} \left( \frac{N}{\zeta(3)} \right)^{1/3} \\ &= 0.94 \hbar \omega_{\text{ho}} N^{1/3}. \end{aligned} \quad (3.18)$$

The condensate fraction is derived by inserting Eq. (3.18) into Eq. (3.17)

$$\frac{N_0}{N} = 1 - \left( \frac{T}{T_c} \right)^3, \quad \text{for } T < T_c. \quad (3.19)$$

Below critical temperature and in the thermodynamic limit, the density of thermal particles is calculated from

$$n_T(\mathbf{r}) = \int \frac{dp}{(2\pi\hbar)^3} \frac{1}{\exp\{\beta\varepsilon(\mathbf{p}, \mathbf{r})\} - 1}, \quad (3.20)$$

where  $\varepsilon(\mathbf{r}, \mathbf{p}) = p^2/2m + V_{\text{ext}}(\mathbf{r})$ . The result is

$$n_T(\mathbf{r}) = \lambda_T^{-3} g_{3/2}(e^{-\beta V_{\text{ext}}(\mathbf{r})}), \quad (3.21)$$

where  $\lambda_T$  is the thermal wavelength and

$$g_{3/2}(z) = \sum_{n=1}^{\infty} z^n / n^{3/2}. \quad (3.22)$$

Though ideal gas model give a good agreement with experimental results, a more quantitative comparison requires the inclusion of the interaction between the particles in the system.

## 3.2 The Interacting Case

The inclusion of interaction is demonstrated, in this section, to give a much more accurate prediction. Using the mean field approach, which its validity shown

to be fitted for dilute Bose gases since the depletion of condensate is about 1% or less.

Starting from a many-body Hamiltonian in second quantization notation

$$\begin{aligned} \hat{H} = & \int d\mathbf{r} \hat{\Psi}^\dagger(\mathbf{r}) \left[ -\frac{\hbar^2}{2m} \nabla^2 + V_{\text{ext}}(\mathbf{r}) \right] \hat{\Psi}(\mathbf{r}) \\ & + \frac{1}{2} \int d\mathbf{r} d\mathbf{r}' \hat{\Psi}^\dagger(\mathbf{r}) \hat{\Psi}^\dagger(\mathbf{r}') V(\mathbf{r}' - \mathbf{r}) \hat{\Psi}(\mathbf{r}') \hat{\Psi}(\mathbf{r}) \end{aligned} \quad (3.23)$$

where  $\hat{\Psi}(\mathbf{r})$  and  $\hat{\Psi}^\dagger(\mathbf{r})$  are the boson field operators that annihilate and create a particle at the position  $\mathbf{r}$ , respectively, and  $V(\mathbf{r}' - \mathbf{r})$  is the two-body interaction potential.

This Hamiltonian can be used to calculate directly the static as well as thermodynamic properties. Though it can give the exact results within the statistical error, as  $N$  becomes larger, the calculation can be heavy or even impractical. Mean-field approach shown to overcome this hindrance. Also it allows one to understand the behavior of the system in terms of a set of parameters having a clear physical meaning.

This approach was first formulated by Bogoliubov [39] to describe the superfluidity phenomenon. This is done by separating the condensate contribution and considering this condensate operator to be a  $c$ -number:  $a_0 = a_0^\dagger = \sqrt{N_0}$ . This is possible since  $N_0$  is large as compared with unity, the expression

$$a_0 a_0^\dagger - a_0^\dagger a_0 = 1 \quad (3.24)$$

is small compared with  $a_0, a_0^\dagger$  themselves.

The field operator can now be

$$\begin{aligned}\hat{\Psi}(\mathbf{r}) &= a_0\phi_0(\mathbf{r}) + \sum_{i=1}^N a_i\phi_i(\mathbf{r}) \\ &= \Phi(\mathbf{r}) + \hat{\Psi}'(\mathbf{r}),\end{aligned}\quad (3.25)$$

here  $\Phi(\mathbf{r}, t)$  is a complex function defined as the expectation value of the field operator  $\Phi(\mathbf{r}, t) \equiv \langle \hat{\Psi}(\mathbf{r}, t) \rangle$ . The function  $\Phi(\mathbf{r}, t)$  is a classical field having the meaning of an order parameter and is often called “the condensate wavefunction”. The condensate wavefunction characterized the off-diagonal long range behavior of the one-body density matrix

$$\rho(\mathbf{r}', \mathbf{r}) = \langle \hat{\Psi}^\dagger(\mathbf{r})\hat{\Psi}(\mathbf{r}') \rangle. \quad (3.26)$$

The density matrix takes a separable form  $\rho(\mathbf{r}, \mathbf{r}') = N\phi_0^*(\mathbf{r}')\phi_0(\mathbf{r})$  which remain different from zero for macroscopic distance

$$\lim_{|\mathbf{r}'-\mathbf{r}|\rightarrow\infty} \rho(\mathbf{r}', \mathbf{r}, t) = \Phi^*(\mathbf{r}', t)\Phi(\mathbf{r}, t). \quad (3.27)$$

In order to derive the equation for condensate wavefunction  $\Phi(\mathbf{r}, t)$  the time evolution of the field operator  $\hat{\Psi}(\mathbf{r}, t)$  can be written by using Heisenberg equation with the many-body Hamiltonian

$$\begin{aligned}i\hbar\frac{\partial}{\partial t}\hat{\Psi}(\mathbf{r}, t) &= [\hat{\Psi}(\mathbf{r}, t), \hat{H}] \\ &= \left[ -\frac{\hbar^2\nabla^2}{2m} + V_{\text{ext}}(\mathbf{r}) \right] \hat{\Psi}(\mathbf{r}, t) \\ &\quad + \left[ \int \hat{\Psi}^\dagger(\mathbf{r}', t)V(\mathbf{r}' - \mathbf{r})\hat{\Psi}(\mathbf{r}', t) d\mathbf{r}' \right] \hat{\Psi}(\mathbf{r}, t).\end{aligned}\quad (3.28)$$

Since the depletion of the condensate is small, the field operator can be replaced by the classical field  $\Phi$ . In the integral containing atom-atom interaction,

$V(\mathbf{r}' - \mathbf{r})$ , this replacement is a poor approximation when short distances ( $\mathbf{r}' - \mathbf{r}$ ) are involved. In the dilute system the binary collisions are dominate the scenario. So one can replace an interaction term by psuedopotential (see Appendix B) in which the strength depend on the  $s$ -wave scattering length which can be express as follow

$$V(\mathbf{r}' - \mathbf{r}) \cong g\delta(\mathbf{r}' - \mathbf{r}) \quad (3.29)$$

where

$$g = \frac{4\pi\hbar^2 a}{m}, \quad (3.30)$$

$a$  is the  $s$ -wave scattering length.

This approximation is compatible with the replacing of  $\hat{\Psi}(\mathbf{r}, t)$  by  $\Phi(\mathbf{r}, t)$ . Finally it gives

$$i\hbar\frac{\partial}{\partial t}\Phi(\mathbf{r}, t) = \left(-\frac{\hbar^2\nabla^2}{2m} + V_{\text{ext}}(\mathbf{r}) + g|\Phi(\mathbf{r}, t)|^2\right)\Phi(\mathbf{r}, t). \quad (3.31)$$

This equation is known as Gross-Pitaevskii equation which was derived separately by E.P. Gross [40, 41] and by L. Pitaevskii [42]. Its validity is based on the conditions that the  $s$ -wave scattering length must be smaller than the interatomic distance and  $N$  is much larger than unity.

There is an alternative way to derive the GP equation. This is done by variational procedure (see Appendix C)

$$i\hbar\frac{\partial}{\partial t}\Phi = \frac{\delta E}{\delta\Phi^*}, \quad (3.32)$$

where the energy functional  $E$  is given by

$$E[\Phi] = \int d\mathbf{r} \left[ \frac{\hbar^2}{2m}|\nabla\Phi|^2 + V_{\text{ext}}(\mathbf{r})|\Phi|^2 + \frac{g}{2}|\Phi|^4 \right]. \quad (3.33)$$



GP equation provides us a tool to investigate static and dynamic properties of Bose-Einstein condensate in a cold dilute gas. It should be noted that due to the assumption  $\hat{\Psi}' \equiv 0$ , the formalism is strictly valid only in the limit of zero temperature.

To obtain a stationary solution, one can write the solution in the form

$$\Phi(\mathbf{r}, t) = e^{-i\mu t/\hbar} \phi(\mathbf{r}). \quad (3.34)$$

Applied this solution to GP equation Eq. (3.31) then time-independent GP equation can now be written as

$$\left[ -\frac{\hbar^2 \nabla^2}{2m} + V_{\text{ext}}(\mathbf{r}) + g\phi^2(\mathbf{r}) \right] \phi(\mathbf{r}) = \mu\phi(\mathbf{r}). \quad (3.35)$$

The  $s$ -wave scattering length entering in the interaction term may be negative or positive correspond to the effective attraction or repulsion, respectively. For a noninteracting case, the condensate has a form of a Gaussian of average width  $a_{\text{ho}}$ , and the central density is proportional to  $N$ . When the interaction has taken into account the scenario is changed. The shape of condensate is decreased(increased) when the value of  $a$  is positive(negative), with respect to the Gaussian (see Fig. 3.1 and Fig. 3.2). The change can be dramatic when the interaction energy is much greater than the kinetic energy, that is, when  $N|a|/a_{\text{ho}} \gg 1$ .

This parameter is obtained by comparing the interaction versus kinetic energy. The first estimation is done by calculating the interaction energy on the ground state of the harmonic oscillator. This energy is given by  $gN\bar{n}$ , where the average density is of the order of  $N/a_{\text{ho}}^3$  so that  $E_{\text{int}} \propto N^2|a|/a_{\text{ho}}^3$ . On the other

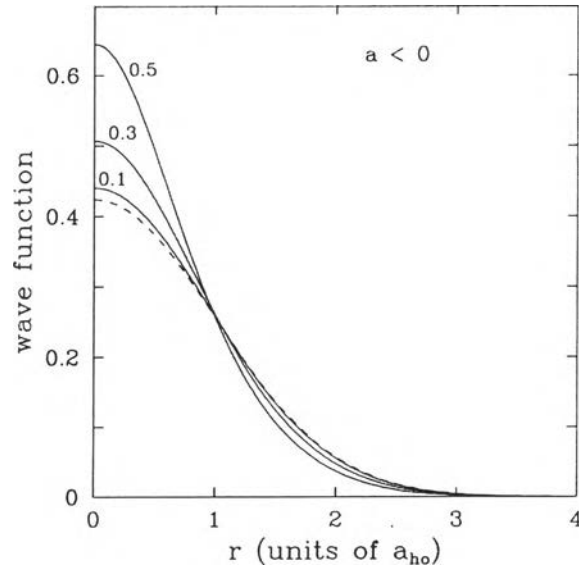


Figure 3.1: Condensate wave function, at  $T = 0$ , obtained by solving numerically the stationary GP equation (Eq. (3.35)) in a spherical trap and with attractive interaction among the atoms ( $a < 0$ ). The three solid lines correspond to  $N|a|/a_{\text{ho}} = 0.1, 0.3, 0.5$ . The dashed line is the prediction for the ideal gas. Here the radius,  $r$ , is in units of the oscillator length  $a_{\text{ho}}$  and plot  $(a_{\text{ho}}^3/N)^{1/2}\phi(r)$  on the vertical axis, so that the curves are normalized to 1, from [43].

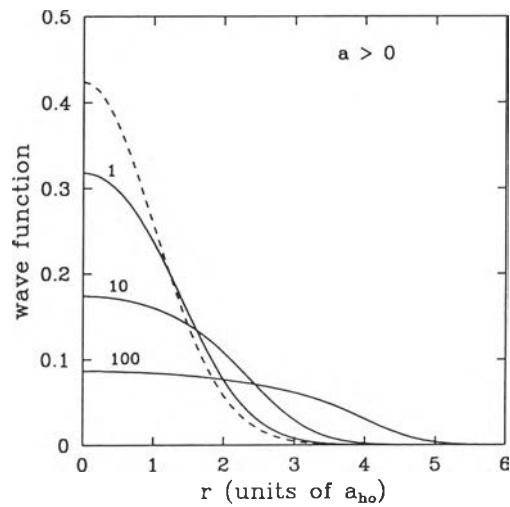


Figure 3.2: Condensate wave function, at  $T = 0$ , obtained by solving numerically the stationary GP equation (Eq. (3.35)) in a spherical trap and with repulsive interaction among the atoms ( $a > 0$ ). The three solid lines correspond to  $N|a|/a_{\text{ho}} = 1, 10, 100$ . The dashed line is the prediction for the ideal gas. Here the radius,  $r$ , is in units of the oscillator length  $a_{\text{ho}}$  and plot  $(a_{\text{ho}}^3/N)^{1/2}\phi(r)$  on the vertical axis, so that the curves are normalized to 1, from [43].

hand, the kinetic energy is of the order of  $N\hbar\omega_{\text{ho}}$  and thus  $E_{\text{kin}} \propto Na_{\text{ho}}^{-2}$ . One finally finds

$$\frac{E_{\text{int}}}{E_{\text{kin}}} \propto \frac{N |a|}{a_{\text{ho}}}. \quad (3.36)$$

The numerical solution of the GP equation for the ground state wave functions with the repulsive interactions have been obtained by a variety of groups for both the isotropic case [44, 45, 46] and the anisotropic case [47, 48, 49]. Compared to the bare harmonic oscillator ground state wavefunction; the wavefunction for the condensate is broaden in space as a result of interactions and its shape deviates markedly from a Gaussian, with a much flatter density profile in the central region for sufficiently large  $N$ . The broaden increases as  $N$  increases, and for an anisotropic case, the extent of broadening is greatest in directions where the restoring forces are weakest. Fig. 3.3 illustrates these features for a  $^{87}\text{Rb}$  condensate.

By direct integration of the stationary GP Equation (3.35), one finds the useful expression

$$\mu = (E_{\text{kin}} + E_{\text{ho}} + 2E_{\text{int}})/N \quad (3.37)$$

for the chemical potential in terms of the different contributions to the energy function Eq. (3.33). Another important expression derived by applying the virial theorem

$$\frac{\langle p_x^2 \rangle}{2m} - \frac{m\omega_x}{2} \langle x^2 \rangle + \frac{1}{2} E_{\text{int}} = 0, \quad (3.38)$$

and similarly for  $y$  and  $z$ . By summing over the three directions one finally finds

$$2E_{\text{kin}} - 2E_{\text{ho}} + 3E_{\text{int}} = 0. \quad (3.39)$$

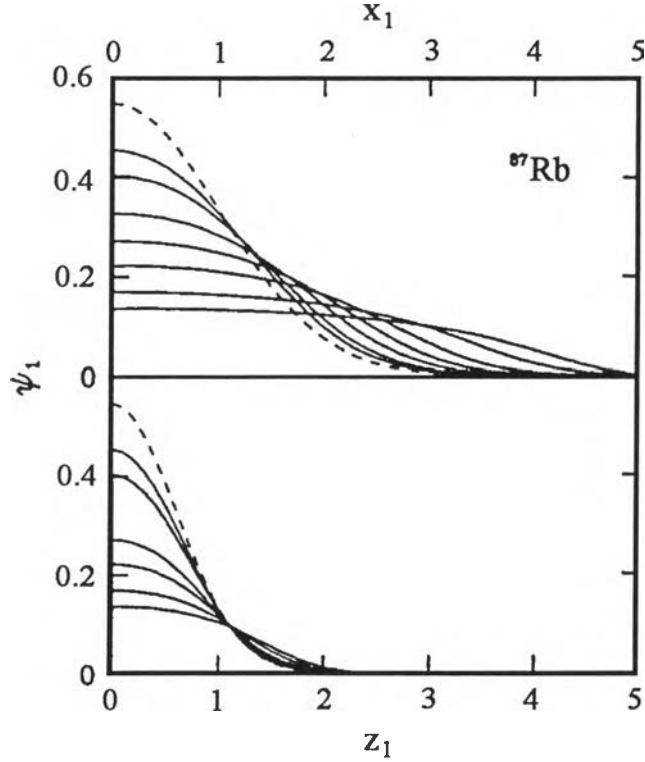


Figure 3.3: Ground state wavefunction for  $^{87}\text{Rb}$  along the  $x$  axis (upper part) and  $z$  axis (lower part). Distances are in units of  $a_{\text{ho}} = (\hbar/m\omega_{\text{ho}})^{1/2}$ , with  $\omega_x = \omega_y = \omega_{\text{ho}}$  and  $\omega_z = \sqrt{8}\omega_{\text{ho}}$ . The dashed line is for noninteracting atoms; the solid lines correspond to  $N = 100, 200, 500, 1000, 2000, 5000, 10^4$ , in descending order of central density, from Dalfovo and Stringari [49].

As  $N$  increases, the interaction energy increases and the repulsion interaction pushes the cloud to the region where trapping potential is higher, thus increasing  $E_{\text{ho}}$ . Conversely, the kinetic energy decreases. Dalfovo and Stringari [49] have explicitly demonstrated this aspect in their numerical results ( see Table 3.1).

In the experiment done by Wieman's group when the trapping potential is suddenly switched off, the cloud is allowed to expand. The image of the cloud has been taken via light absorption technique. Also the velocity distribution is obtained and by integrating over the distribution the kinetic energy of the system is obtained. This energy, which is called *release energy*, coincides with the sum

$N$	$\mu_1$	$(E_1/N)$	$(E_1/N)_{\text{kin}}$	$(E_1/N)_{\text{ho}}$	$(E_1/N)_{\text{int}}$
1	2.414	2.414	1.207	1.207	0.000
100	2.88	2.66	1.06	1.39	0.21
200	3.21	2.86	0.98	1.52	0.36
500	3.94	3.30	0.86	1.81	0.63
1000	4.77	3.84	0.76	2.15	0.93
2000	5.93	4.61	0.66	2.64	1.32
5000	8.14	6.12	0.54	3.57	2.02
10000	10.5	7.76	0.45	4.57	2.74
15000	12.2	8.98	0.41	5.31	3.26
20000	13.7	9.98	0.38	5.91	3.68

Table 3.1: Results for the ground state of  $^{87}\text{Rb}$  atoms in a trap with  $\lambda = \sqrt{8}$ . The subscript kin., ho., and int. refer to kinetic, harmonic and interaction energy.  $\mu_1$  and  $E_1$  are chemical potential and energy are in units  $\hbar\omega_{\perp}$ , with  $\omega_z/2\pi = 220$  Hz. Length is in units  $a_{\perp}$ , from [49].

of the kinetic and interaction energies at the beginning of the expansion since at that instant the harmonic potential was excluded:

$$E_{\text{rel}} = E_{\text{kin}} + E_{\text{int}}. \quad (3.40)$$

Since energy is conserved during the expansion, its initial value, calculated with the stationary GP equation, can be directly compared with experiments.

From the comparison, it shows the evidence for the crucial role played by two-body interactions. The noninteracting case gives  $E_{\text{rel}}/N = \frac{1}{2} \left(1 + \frac{\lambda}{2}\right) \hbar\omega_{\text{ho}}$ , independent of  $N$ . In contrast the interacting model gives a good agreement with the observed release energy which depends rather strongly on  $N$ . Fig. 3.4 and Fig. 3.5 show the data obtained at JILA [50] and MIT [23] respectively.

Contrasting to the noninteracting case, now consider the situation where the interaction is strong. This can be achieved when  $N$  is increased so that the parameter  $N|a|/a_{\text{ho}}$  is much larger than unity. The effect of strong repulsive interaction is that atoms are pushed outwards. The condensate wavefunction become

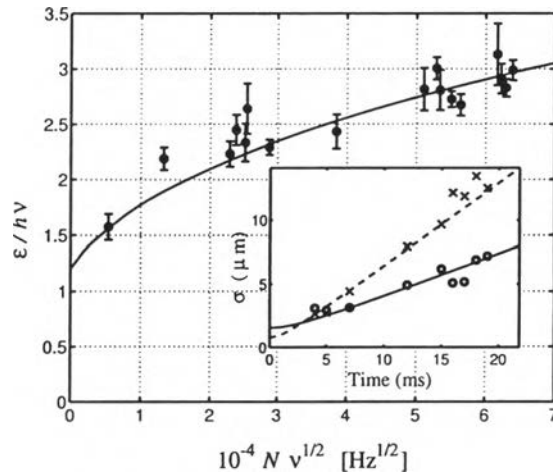


Figure 3.4: Comparison of the release energy as a function of interaction strength from the stationary GP equation (solid line) and the experimental measurements (solid circles). Inset shows the expansion of widths of the condensate in the horizontal (empty circles) and vertical (crosses) directions against the predictions of the time dependent GP equation (dashed and solid lines) for the data point at  $10^{-4} N \nu^{1/2} = 0.53$ . Here  $\nu$  is the frequency of the trapping potential and the trapped gas is rubidium. From Holland *et al.* [50].

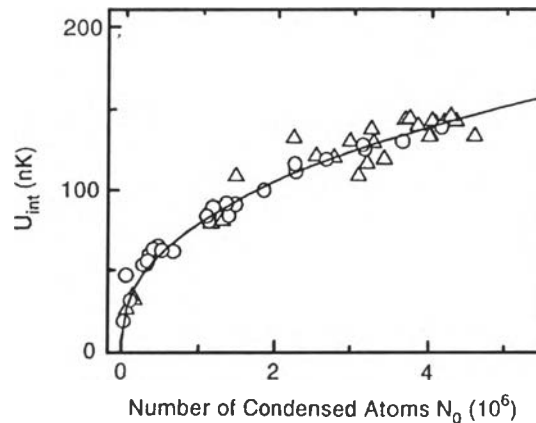


Figure 3.5: Release energy of the condensate as a function of the number of condensed atoms in the MIT trap with sodium atoms. For these condensates the initial kinetic energy is negligible and the release energy coincides with the mean-field energy. The symbol  $U_{int}$  is here used for the mean-field energy per particle. Triangles: clouds with no visible thermal component. Circles: clouds with both thermal and condensed fractions visible. The solid line is a fit proportional to  $N_0^{2/5}$ . From Mewes *et al.* [23].

rather flat at center of the trap. Consequently the gradient of the condensate is small compare to others terms and can be neglected. Now the solution of the stationary GP Equation (3.35) takes the form

$$\phi(\mathbf{r}) = \left[ \frac{m}{4\pi\hbar^2 a} \{ \mu - V_{\text{ext}}(\mathbf{r}) \} \right]^{1/2}, \quad (3.41)$$

which provides the accurate description of the exact solution in the interior of the atomic cloud. This approximation is known as Thomas-Fermi which is opposed to the noninteracting limit.

The normalization condition provides the relation between chemical potential and number of particles:

$$\mu = \frac{\hbar\omega_{\text{ho}}}{2} \left( \frac{15Na}{a_{\text{ho}}} \right)^{2/5}. \quad (3.42)$$

Moreover, since  $\mu = \partial E / \partial N$ , the energy per particle turns out to be  $E/N = (5/7)\mu$ . Finally, in the large  $N$  limit, the release energy coincides with the interaction energy:  $E_{\text{rel}}/N = (2/7)\mu$ .

The chemical potential, as well as the interaction and oscillator energies obtained by solving numerically the stationary GP Equation (3.35) become closer and closer to the Thomas-Fermi values when  $N$  increases ( see for instance, [49]). For sodium atoms in the MIT traps, where  $N$  is larger than  $10^6$ , the Thomas-Fermi approximation is practically indistinguishable from the solution of GP equation. The release energy per particle measured by [23] is indeed well fitted with a  $N^{2/5}$  law, as shown in Fig. 3.5.

The Gross-Pitaevskii equation cannot be solved analytically and even numerical solution is difficult or impractical to obtain when the number of particle

is large. It is therefore sensible to attempt approximation solutions, in order to obtain some physical insight and a qualitative understanding of the condensate behavior. One approach is a variational method [51]. In this approach the wavefunction can be applied over the range of interaction. Still, it requires one to fit parameters in the solution with the result obtained by experiments. The reasonable choice for the trial wavefunction to be the form of the lowest single particle mode and now the trapping frequencies is interpreted as variational parameters, as

$$\phi(\mathbf{r}) = N^{1/2} \Omega_{\perp}^{1/2} \Omega_z^{1/4} \left( \frac{m}{\pi \hbar} \right)^{3/4} e^{-m(\Omega_{\perp} r_{\perp}^2 + \Omega_z z^2)/2\hbar} \quad (3.43)$$

where  $\Omega_{\perp}$  and  $\Omega_z$  are the effective frequencies treated as variational parameters. Substituting Eq. (3.43) into Eq. (3.33) yields the ground state energy

$$E(\Omega_{\perp}, \Omega_z) = N \hbar \left( \frac{\Omega_{\perp}}{2} + \frac{\omega_{\perp}^2}{2\Omega_{\perp}} + \frac{\Omega_z}{4} + \frac{\omega_z^2}{4\Omega_z} + Na \Omega_{\perp} \Omega_z^{1/2} \left( \frac{m}{2\pi \hbar} \right)^{1/2} \right). \quad (3.44)$$

In the attractive interaction case, which corresponds to a negative value of scattering length, the central density of the cloud increases rapidly with  $N$ . This is the effect of adding more and more attractive interaction energy. In the inhomogeneous gas this effect is counterbalanced by the zero point kinetic energy, often called quantum pressure. It should be noted that in the homogeneous case the quantum pressure is absent hence the condensate is always unstable. As the number of particles increases to some definite degree the attractive force surpasses the quantum pressure. Consequently the condensate is unstable. This implies that for the attractive interaction the number of particles participating in the cloud is limited.

The limiting number of particles  $N_{cr}$  can be calculated at zero temperature by means of the Gross-Pitaevskii equation. It is obvious from the energy functional that



there is no global minimum. Fortunately the quantum pressure when exceed the interaction can produce the local minimum. Fig. 3.1 shows the condensate corresponding to local minimum for different  $N$ . As  $N$  increases the depth of the local minima decreases. Above the critical value the local minima is no longer exist and GP equation has no solution. In the spherical trap the critical value is [46]

$$N_{\text{cr}} = 0.575 \frac{a_{\text{ho}}}{|a|}. \quad (3.45)$$

For axially symmetric trap with  ${}^7\text{Li}$  used in [52, 53, 54] the numerical result predicts  $N_{\text{cr}} \simeq 1400$  [49, 55] which is consistent with the measurements made by [53, 54].

Again the variational method is applied to obtain an insight of the condensate. For a spherical trap one can minimized the energy functional Eq. (3.33) using the trial wavefunction

$$\phi(\mathbf{r}) = \left( \frac{N}{\varpi^3 a_{\text{ho}}^3 \pi^{3/2}} \right)^{1/2} \exp\left( \frac{-r^2}{2\varpi^2 a_{\text{ho}}^2} \right). \quad (3.46)$$

where  $\varpi$  is a dimensionless variational parameter which fixes the width of the condensate. One gets

$$\frac{E(\varpi)}{N\hbar\omega_{\text{ho}}} = \frac{3}{4} (\varpi^{-2} + \varpi^2) - (2\pi)^{-1/2} \frac{N|a|}{a_{\text{ho}}} \varpi^{-3}. \quad (3.47)$$

This energy is plotted in Fig. 3.6 as a function of  $\varpi$ , for several values of the parameter  $N|a|/a_{\text{ho}}$ . It is obvious that the local minima disappears when this parameter surpass the critical value. To determine the critical number of particle, one requires that

$$\frac{dE}{d\varpi} = \frac{d^2E}{d\varpi^2} = 0. \quad (3.48)$$

Thus one obtains

$$N_{\text{cr}} \simeq 0.67 \frac{a_{\text{ho}}}{|a|}, \quad (3.49)$$

about 20% greater than the value obtained numerically. The comparison give a measure of the accuracy of the Gaussian wavefunction approximation.

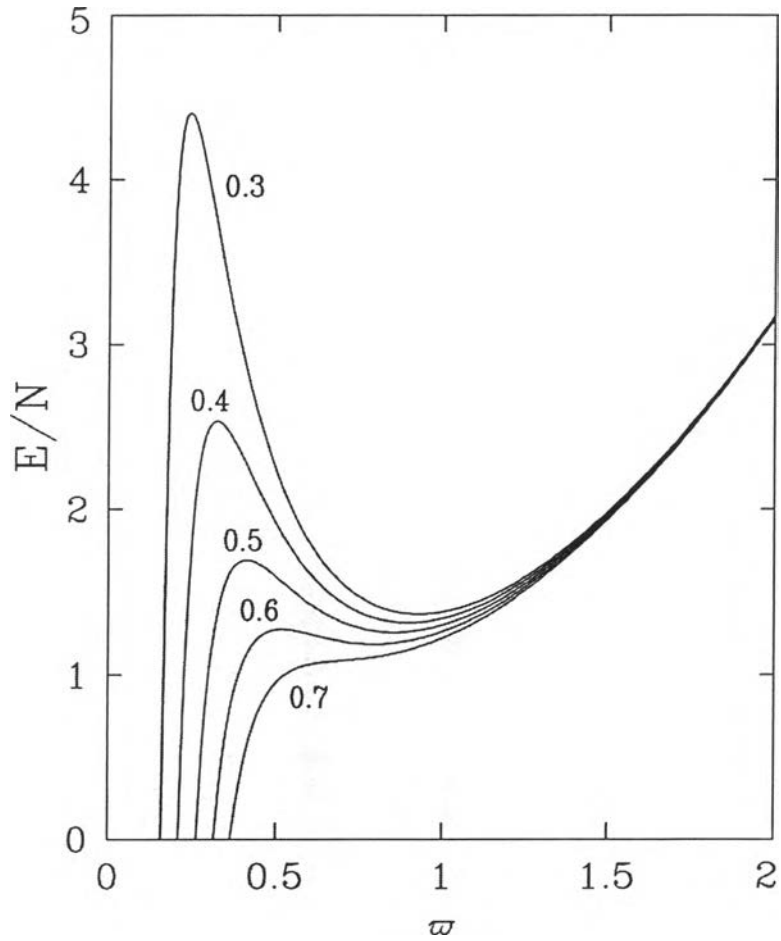


Figure 3.6: Energy per particle, in units of  $\hbar\omega_{\text{ho}}$ , for atoms in a spherical trap interacting with attractive forces, as a function of the effective width  $w$  in the Gaussian model of Eq. (3.46) - Eq. (3.47). Curves are plotted for several values of the parameter  $N|a|/a_{\text{ho}}$ . The local minimum disappears at  $N = N_{\text{cr}}$ , from [43].